

Conjugated Pyridines with an End-Capping Ferrocene

Jiann T. Lin,* Jiann Jung Wu, Chyi-Shiun Li, Yuh S. Wen, and Kuan-Jiuh Lin

Institute of Chemistry, Academia Sinica, Nankang, Taipei, Taiwan, Republic of China

Received July 22, 1996[®]

This study reports the synthesis of new pyridyl ligands incorporating an alkyne entity with an end-capping ferrocenyl moiety: 1-(ferrocenylethynyl)-4-((4-pyridyl)ethynyl)benzene (FEPEB), 1-ferrocenyl-6-(4-pyridyl)hexatriyne (FPHT), and 1-ferrocenyl-4-(4-pyridyl)-butadiyne (FPBD). The complexes $W(CO)_4(L)(FEPEB)$ ($L = CO, PPh_3, P(OMe)_3, PMe_3$), $W(CO)_4(L)(FPHT)$ ($L = CO, PPh_3, P(OMe)_3, PMe_3$), and $W(CO)_5(FPBD)$ are obtained by ligating FEPEB, FPHT, and FPBD to $W(CO)_4(L)(THF)$. The energy of tungsten metal to pyridyl π^* charge transfer (MLCT) depends on both the pyridyl ligand and the ancillary ligand, L. Treating FPHT and FPBD with MeI causes *N*-methylpyridinium derivatives to form, which exhibit a strong low-lying charge-transfer band. As a comparative study, the complexes 1-(ferrocenylethynyl)-4-((4-nitrophenyl)ethynyl)-benzene (FENEb) and 1-(ferrocenylethynyl)-4-((4-aminophenyl)ethynyl)benzene (FEAEb) have also been synthesized. X-ray analysis has been employed to examine the structures of 1-(ferrocenylethynyl)-4-ethynylbenzene, $W(CO)_4(PPh_3)(FEPEB)$, $W(CO)_5(FPHT)$, and 1,8-diferrocenyloctatetrayne.

Introduction

The study of dinuclear complexes linked by conjugated pyridyl ligands is an intriguing area of research, not least for the possibilities they offer of electronic communication between terminal subunits.¹ Our interest in di- and polynuclear metal complexes bridged by pyridyl ligands incorporating an alkyne entity² has focused on several potential aspects of application: (a) the complexes may exhibit nonlinear optical phenomena³ because the metal fragment can function either as an electron donor,⁴ due to strong metal to ligand charge transfer (MLCT),⁵ or as an electron acceptor, on the basis of the σ -donation from the nitrogen atom to the metal center;⁶ (b) a molecule can retain two or more metal centers,⁷ providing a cooperative effect in catalysis; (c) metal organic polymers can be derived from these organometallic complexes;⁸ (d) bridged dinuclear complexes may serve as models for investigating metal–metal interaction.⁹

Our previous papers reported dinuclear tungsten carbonyl and rhenium carbonyl complexes with a pyridyl bridge incorporating an alkyne entity.² Our continuing inquiries now turn to how the metal moieties as well as the bridges in these systems may be varied. In view of the high stability and redox-active properties of ferrocene,¹⁰ this study extends the interest to the analogous pyridyl ligand bridged complexes in which an electron-releasing ferrocenyl group¹¹ is one of the terminal subunits. This following work investigates the syntheses and certain physical properties of these new complexes.

Experimental Section

The general procedures and physical measurements resemble those described in an earlier report.² 4-Ethynylpyridine,¹² 1,4-diethynylbenzene,¹³ 1-iodoferrocene,¹⁴ ferrocen-

* To whom correspondence should be addressed. E-mail: jtlin@chem.sinica.edu.tw.

[®] Abstract published in *Advance ACS Abstracts*, October 15, 1996.

(1) (a) Thomas, J. A.; Hutchings, M. G.; Jones, C. J.; McCleverty, J. A. *Inorg. Chem.* **1996**, *35*, 289. (b) McWhinnie, S. L. W.; Thomas, J. A.; Hamor, T. A.; Jones, C. J.; McCleverty, J. A.; Collison, D.; Mabbs, F. E.; Harding, C. J.; Yellowlees, L. J.; Hutchings, M. G. *Inorg. Chem.* **1996**, *35*, 760. (c) Hissler, M.; Ziessel, R. *J. Chem. Soc., Dalton Trans.* **1995**, 893. (d) Harriman, A.; Hissler, M.; Ziessel, R.; Cian, A. D.; Fisher, J. *J. Chem. Soc., Dalton Trans.* **1995**, 4067.

(2) (a) Lin, J. T.; Sun, S. S.; Wu, J. J.; Liaw, Y. C.; Lin, K. J. *J. Organomet. Chem.* **1996**, *517*, 217. (b) Lin, J. T.; Sun, S. S.; Wu, J. J.; Lee, L. S.; Lin, K. J.; Huang, Y. F. *Inorg. Chem.* **1995**, *34*, 2323.

(3) Long, N. J. *Angew. Chem., Int. Ed. Engl.* **1995**, *34*, 21.

(4) (a) Kanis, D. R.; Ratner, M. A.; Marks, T. J. *Chem. Rev.* **1994**, *94*, 195. (b) Bourgault, M.; Tam, W.; Eaton, D. F. *Organometallics* **1990**, *9*, 2856.

(5) Geoffroy, G. L.; Wrighton, M. S., Eds. *Organometallic Photochemistry*; Academic Press: New York, 1979.

(6) (a) Kanis, D. R.; Lacroix, P. G.; Ratner, M. A.; Marks, T. J. *J. Am. Chem. Soc.* **1994**, *116*, 10089. (b) Bourgault, M.; Mountassir, C.; Le Bozec, H.; Ledoux, I.; Pucetti, G.; Zys, J. *J. Chem. Soc., Chem. Commun.* **1993**, 1623.

(7) (a) Bunz, U. H. F.; Enkelmann, V.; Räder, J. *Organometallics* **1993**, *12*, 4745. (b) Wiegelmann, J. E. C.; Bunz, U. H. F. *Organometallics* **1993**, *12*, 3792. (c) Sterzo, C. L.; Stille, J. K. *Organometallics* **1990**, *9*, 687. (d) Sterzo, C. L.; Miller, M. M.; Stille, J. K. *Organometallics* **1989**, *8*, 2331.

(8) (a) Jia, G.; Puddephatt, R. J.; Vittal, J. J.; Payne, N. C. *Organometallics* **1993**, *12*, 263. (b) Zeldih, M.; Wynne, K.; Allcock, H. R., Eds. *Inorganic and Organometallic Polymers*; Advances in Chemistry Series 224; American Chemical Society: Washington, DC, 1988.

(9) (a) Grosshenny, V.; Ziessel, R. *J. Chem. Soc., Dalton Trans.* **1993**, 817. (b) Das, A.; Maher, J. P.; McCleverty, J. A.; Badiola, J. A. N.; Ward, M. D. *J. Chem. Soc., Dalton Trans.* **1993**, 681. (c) Potts, K. T.; Horwitz, C. P.; Fessak, A.; Kesharar, K. M.; Nash, K. E.; Toscano, P. J. *J. Am. Chem. Soc.* **1993**, *115*, 10444. (d) Bunel, E. E.; Valle, L.; Jones, N. L.; Carroll, P. J.; Gonzalez, M.; Munoz, N.; Manriquez, J. M. *Organometallics* **1988**, *7*, 789. (e) Sutton, J. E.; Taube, H. *Inorg. Chem.* **1981**, *20*, 3125.

(10) Togni, A.; Hayashi, T., Eds. *Ferrocenes*; VCH: Weinheim, Germany, 1995.

(11) (a) Togni, A.; Rins, G. *Organometallics* **1993**, *12*, 3368. (b) Doineau, G.; Balavoine, G.; Fillebeen-Khan, T.; Clinet, J. C.; Delaire, J.; Ledoux, I.; Loucif, R.; Pucetti, G. *J. Organomet. Chem.* **1991**, *421*, 299. (c) Green, M. L. H.; Qin, J.; O'Hare, D.; Bunting, H. E.; Thompson, M. E.; Marder, S. R.; Chatakond, K. *Pure Appl. Chem.* **1989**, *61*, 817. (d) Green, M. L. H.; Marder, S. R.; Thompson, M. E.; Bandy, J. A.; Bloor, D.; Kolinsky, P. V.; Jones, R. J. *Nature* **1987**, *330*, 360.

(12) King, R. B., Ed. *Organometallic Synthesis, Transition-Metal Compounds*; Academic Press: New York, 1965; Vol. 1.

(13) Austin, W. B.; Bilow, N.; Kelleghan, W. J.; Lau, K. S. *J. Org. Chem.* **1981**, *46*, 2280.

(14) Jones, K.; Lappert, M. F. *J. Organomet. Chem.* **1965**, *3*, 295.

ylacetylene,¹⁵ and ferrocenylbutadiyne¹⁶ have been prepared as described previously.

1-(Ferrocenylethynyl)-4-ethynylbenzene (1). A 14.9 mL amount of *n*-BuLi (1.6 M in hexane, 23.8 mmol) was added over a 20 min period to a THF solution of 1,4-diethynylbenzene (3.0 g, 23.8 mmol) prechilled to $-70\text{ }^{\circ}\text{C}$. After 1 h, a THF solution of ZnCl_2 (3.24 g, 23.8 mmol) was added; the mixture was warmed to room temperature and stirred for a further 1 h. The solution was then added to a mixture of iodoferrrocene (7.40 g, 23.8 mmol) and $\text{Pd}(\text{PPh}_3)_4$ (820 mg, 0.71 mmol); after 24 h, this mixture was pumped dry and the residue extracted with $\text{Et}_2\text{O}/\text{H}_2\text{O}$. Then, the ether layer was pumped dry and the residue chromatographed. Elution by $\text{CH}_2\text{Cl}_2/\text{hexane}$ (1:3) caused two bands to appear. The first was unreacted iodoferrrocene, and from the second, pale red-orange powdery **1** was obtained in 37% yield (2.70 g). MS (FAB): *m/e* 310 (M^+). Anal. Calcd for $\text{C}_{20}\text{H}_{14}\text{Fe}$: C, 77.45; H, 4.55. Found: C, 77.21; H, 4.28.

1-(Ferrocenylethynyl)-4-((4-pyridyl)ethynyl)benzene (2; FEPEB). Et_2NH (100 mL) was added to a flask containing a mixture of 4-bromopyridine hydrochloride (1.88 g, 9.8 mmol), **1** (2.50 g, 8.1 mmol), $\text{Pd}(\text{PPh}_3)_2\text{Cl}_2$ (270 mg, 0.24 mmol), and CuI (45 mg, 0.24 mmol). The resulting mixture was heated to $60\text{--}65\text{ }^{\circ}\text{C}$ for 24 h. The solvent was removed in vacuo and the residue extracted with $\text{Et}_2\text{O}/\text{H}_2\text{O}$. The ether layer was transferred to a flask containing MgSO_4 to remove H_2O and filtered. The filtrate was pumped dry and the residue chromatographed. Elution by THF/hexane (1:5) provided the yellow-orange powdery **2** in 46% yield (1.44 g). MS (FAB): *m/e* 387 (M^+). Anal. Calcd for $\text{C}_{25}\text{H}_{17}\text{NFe}$: C, 77.52; H, 4.43; N, 3.62. Found: C, 77.42; H, 4.18; N, 3.45.

$\text{W}(\text{CO})_4(\text{L})(\text{FEPEB})$ (3, L = CO; 4, L = PPh_3 ; 5, L = $\text{P}(\text{OMe})_3$; 6, L = PMe_3). Essentially the same procedures were applied to synthesize **3–6**; consequently, only the preparation of **4** is described in detail. A THF solution of $\text{W}(\text{CO})_4(\text{PPh}_3)(\text{THF})$ prepared in situ from $\text{W}(\text{CO})_6$ (600 mg, 1.70 mmol) and PPh_3 (446 mg, 1.70 mmol) was reduced in volume and transferred to a flask containing FEPEB. The solution was stirred for 18 h, and the solvent was removed under a vacuum. The residue was chromatographed under nitrogen. Elution by $\text{CH}_2\text{Cl}_2/\text{hexane}$ (1:3) caused a red band to appear, from which a deep red powdery **4** was isolated in 28% yield (450 mg). MS (FAB): *m/e* 946 ($(\text{M} + 1)^+$, ^{184}W). Anal. Calcd for $\text{C}_{47}\text{H}_{32}\text{NO}_4\text{PFeW}$: C, 59.71; H, 3.41; N, 1.48. Found: C, 59.84; H, 3.55; N, 1.32.

The yellow complex **3** was eluted by $\text{CH}_2\text{Cl}_2/\text{hexane}$ (1:6) in a yield of 53%. Anal. Calcd for $\text{C}_{30}\text{H}_{17}\text{NO}_5\text{FeW}$: C, 50.67; H, 2.41; N, 1.97. Found: C, 50.65; H, 2.38; N, 1.81.

The red-orange complex **5** was eluted by $\text{CH}_2\text{Cl}_2/\text{hexane}$ (1:2), giving a yield of 27%. Anal. Calcd for $\text{C}_{32}\text{H}_{26}\text{NO}_7\text{PFeW}$: C, 47.61; H, 3.25; N, 1.74. Found: C, 47.67; H, 3.31; N, 1.57.

The red complex **6** was eluted by $\text{CH}_2\text{Cl}_2/\text{hexane}$ (1:2.5), providing a yield of 25%. Anal. Calcd for $\text{C}_{32}\text{H}_{26}\text{NO}_4\text{PFeW}$: C, 50.62; H, 3.45; N, 1.84. Found: C, 50.52; H, 3.48; N, 1.73.

1-Ferrocenyl-6-(4-pyridyl)hexatriyne (7, FPHT). To a mixture of ferrocenylbutadiyne (1.00 g, 4.27 mmol), ethynylpyridine (0.53 g, 5.12 mmol), $\text{Cu}(\text{OAc})_2 \cdot \text{H}_2\text{O}$ (46 mg, 0.13 mmol), and CuI (24 mg, 0.13 mmol) was added 80 mL of pyridine, 50 mL of Et_2O , and 30 mL of MeOH. The resulting mixture was stirred in air for 18 h. The solvent was removed under vacuum, and the residue was chromatographed under nitrogen. Elution by THF/hexane (1:6) afforded two bands. The first band was identified as 1,8-bis(ferrocenyl)octatetrayne (20%). The pale red-orange powdery **7** was isolated in 35% yield (500 mg) from the second band. MS (FAB): *m/e* 401 (M^+). Anal. Calcd for $\text{C}_{21}\text{H}_{13}\text{NFe}$: C, 75.25; H, 3.91; N, 4.18. Found: C, 75.20; H, 3.90; N, 4.00.

$\text{W}(\text{CO})_4(\text{L})(\text{FPHT})$ (8, L = CO; 9, L = PPh_3 ; 10, L = $\text{P}(\text{OMe})_3$; 11, L = PMe_3). Again, the same procedures were followed for synthesizing **8–11**, and therefore, only the preparation of **9** is described. A THF solution of $\text{W}(\text{CO})_4(\text{PPh}_3)(\text{THF})$ prepared in situ from $\text{W}(\text{CO})_6$ (0.50 g, 1.42 mmol) and PPh_3 (0.38 g, 1.42 mmol) was reduced in volume and transferred to a flask containing FPHT (0.48 g, 1.42 mmol). The solution was stirred for 18 h, and solvent was removed under vacuum. The residue was chromatographed under nitrogen. Elution by $\text{CH}_2\text{Cl}_2/\text{hexane}$ (1:3) provided a red band from which the powdery **9** was isolated in 32% yield (400 mg). MS (FAB): *m/e* 893 (M^+ , ^{184}W). Anal. Calcd for $\text{C}_{43}\text{H}_{28}\text{NO}_4\text{PFeW}$: C, 57.81; H, 3.16; N, 1.57. Found: C, 57.62; H, 3.01; N, 1.30.

The light red complex **8** was eluted by $\text{CH}_2\text{Cl}_2/\text{hexane}$ (1:4) and isolated in 54% yield. Anal. Calcd for $\text{C}_{26}\text{H}_{13}\text{NO}_5\text{FeW}$: C, 47.38; H, 1.99; N, 2.13. Found: C, 47.32; H, 1.93; N, 2.07.

The deep red complex **10** was eluted by $\text{CH}_2\text{Cl}_2/\text{hexane}$ (1:4) and isolated in 29% yield. Anal. Calcd for $\text{C}_{28}\text{H}_{22}\text{NO}_7\text{PFeW}$: C, 44.53; H, 2.94; N, 1.85. Found: C, 44.35; H, 2.86; N, 1.80.

The purple complex **11** was eluted by $\text{CH}_2\text{Cl}_2/\text{hexane}$ (1:4) and isolated in 31% yield. Anal. Calcd for $\text{C}_{28}\text{H}_{22}\text{NO}_4\text{PFeW}$: C, 47.56; H, 3.14; N, 1.98. Found: C, 47.50; H, 3.01; N, 1.83.

1-Ferrocenyl-4-(4-pyridyl)butadiyne (12; FPBD). Compound **12** was synthesized in the same manner employed for **7**, except that ferrocenylacetylene was used instead of ferrocenylbutadiyne. The first band was identified as 1,4-bis(ferrocenyl)butadiyne (15%). The red powdery **12** was isolated in 15% yield from the second band. MS (FAB): *m/e* 311 (M^+). Anal. Calcd for $\text{C}_{19}\text{H}_{13}\text{NFe}$: C, 73.34; H, 4.21; N, 4.50. Found: C, 73.42; H, 4.38; N, 4.79.

$\text{W}(\text{CO})_5(\text{FPBD})$ (13). Complex **13** was synthesized by the same procedures employed for **8–11** except that FPBD served instead of FPHT. A reddish brown complex **13** was eluted by $\text{CH}_2\text{Cl}_2/\text{hexane}$ (1:5) and isolated in 26% yield. Anal. Calcd for $\text{C}_{24}\text{H}_{13}\text{NO}_5\text{FeW}$: C, 45.39; H, 2.06; N, 2.21. Found: C, 45.32; H, 2.10; N, 2.16.

1-Ferrocenyl-6-(1-methyl-4-pyridiniumyl)hexatriyne Iodide (14; FPHTI). To a CH_2Cl_2 solution (50 mL) of **7** (100 mg, 0.299 mmol) was added a 10-fold excess of MeI. The solution was then stirred at room temperature for 16 h. After the solvent was removed, the residue was washed with hexane and dried in vacuo to provide a brown powdery **14** in 56% yield (81 mg). MS (FAB): *m/e* 350 ($(\text{M} - \text{I})^+$). Anal. Calcd for $\text{C}_{22}\text{H}_{16}\text{NFe}$: C, 55.38; H, 3.38; N, 2.94. Found: C, 55.30; H, 3.22; N, 2.80.

1-Ethynyl-4-((4-nitrophenyl)ethynyl)benzene (15). A 7.7 mL portion of *n*-BuLi (1.5 M in THF, 11.6 mmol) was added over a 10 min period to a THF solution of 1,4-diethynylbenzene (1.33 g, 10.6 mmol), prechilled to $-70\text{ }^{\circ}\text{C}$. After 1 h, a THF solution of ZnCl_2 (1.44 g, 10.6 mmol) was added and the mixture warmed to room temperature. The solution was stirred for a further 1 h and then added to a mixture of 4-iodo-1-nitrobenzene (2.63 g, 10.6 mmol) and $\text{Pd}(\text{PPh}_3)_4$ (365 mg, 0.32 mmol). After 24 h, the solution was pumped dry and the residue extracted with $\text{Et}_2\text{O}/\text{H}_2\text{O}$. After the solvent was removed from the ether layer, the pale yellow powdery **15** was isolated in 50% yield (1.30 g). MS (FAB): *m/e* 247 (M^+). Anal. Calcd for $\text{C}_{16}\text{H}_9\text{NO}_2$: C, 77.72; H, 3.67; N, 5.66. Found: C, 77.49; H, 3.37; N, 5.60.

1-(Ferrocenylethynyl)-4-((4-nitrophenyl)ethynyl)benzene (16; FENEB). Et_2NH (100 mL) was added to a flask containing a mixture of iodoferrrocene (1.27 g, 2.02 mmol), **15** (0.50 g, 2.02 mmol), $\text{Pd}(\text{PPh}_3)_2\text{Cl}_2$ (42.5 mg, 0.060 mmol), and CuI (19.2 mg, 0.10 mmol). The solution was then heated to $55\text{--}60\text{ }^{\circ}\text{C}$ for 24 h. The solvent was removed in vacuo and the residue extracted with $\text{Et}_2\text{O}/\text{H}_2\text{O}$. To remove H_2O , the ether layer was transferred to a flask containing MgSO_4 and filtered. The filtrate was pumped dry, and the residue was chromatographed. Elution by $\text{CH}_2\text{Cl}_2/\text{hexane}$ (1:3) yielded two bands. The first was the unreacted iodoferrrocene, and from the second band, after the solvent was removed, red powdery

(15) Rosenblum, M.; Brawn, N.; Papenmeier, J.; Applebaum, M. *J. Organomet. Chem.* **1966**, *6*, 173.

(16) Yuan, Z.; Stringer, G.; Jobe, I. R.; Kreller, D.; Scott, K.; Koch, L.; Taylor, N. J.; Marder, T. B. *J. Organomet. Chem.* **1993**, *452*, 115.

Table 1. Crystal Data for Compounds **1**, **4**, **8**, and **19**

	1	4	8	19
chem formula	C ₂₀ H ₁₄ Fe	C ₄₇ H ₃₁ FeNO ₄ PFeW	C ₂₆ H ₁₃ NO ₅ FeW	C ₁₄ H ₉ Fe
fw	310.17	944.43	659.09	233.07
cryst size, mm	0.25 × 0.09 × 0.06	0.34 × 0.13 × 0.25	0.25 × 0.25 × 0.06	0.25 × 0.25 × 0.25
space group	<i>P2₁/n</i>	<i>P1</i>	<i>P2₁/m</i>	<i>C2/m</i>
<i>a</i> , Å	5.993(2)	12.208(2)	8.321(2)	11.980(2)
<i>b</i> , Å	19.912(3)	12.674(1)	10.106(2)	8.942(2)
<i>c</i> , Å	12.393(2)	13.934(1)	14.411(3)	10.018(4)
α , deg		108.707(7)		
β , deg	98.06(2)	100.63(1)	95.06(2)	106.47(2)
γ , deg		94.7339(9)		
<i>V</i> , Å ³	1464.2(6)	1983.7(4)	1207.2(4)	1029.0(5)
<i>Z</i>	4	2	4	4
<i>T</i> , °C	+25	+25	+25	+25
λ (Mo K α), Å	0.7107	0.7107	0.7107	0.7107
ρ_{calc} , g cm ⁻³	1.407	1.581	3.627	1.504
μ , cm ⁻¹	10.2	34.1	110.0	28.4
transmissn coeff	1.00–0.95	1.00–0.64	1.00–0.48	0.92–0.78
<i>R</i> ^a	0.041	0.031	0.031	0.029
<i>R</i> _w ^b	0.044	0.035	0.033	0.033

^a $R = \sum ||F_o| - |F_c|| / \sum |F_o|$. ^b $R_w = [\sum w(|F_o| - |F_c|)^2 / \sum w|F_o|^2]^{1/2}$; $w = 1/[\sigma^2(F_o) + kF_o^2]$. For **1**, $k = 0.0002$; for **4**, **8**, and **19**, $k = 0.0001$.

16 was obtained in 69% yield (0.60 g). MS (FAB): *m/e* 431 (M⁺). Anal. Calcd for C₂₆H₂₇NO₂Fe: C, 72.39; H, 3.98; N, 3.25. Found: C, 72.15; H, 3.90; N, 3.12.

1-Ethynyl-4-((4-aminophenyl)ethynyl)benzene (17). The same general procedures were followed for synthesizing **15**, except that 4-iodoaniline served instead of 4-iodo nitrobenzene. A pale yellow powdery **17** was isolated in 45% yield (1.50 g). MS (FAB): *m/e* 218 (M⁺). Anal. Calcd for C₁₆H₁₁N: C, 88.13; H, 5.44; N, 6.43. Found: C, 87.95; H, 5.21; N, 6.25.

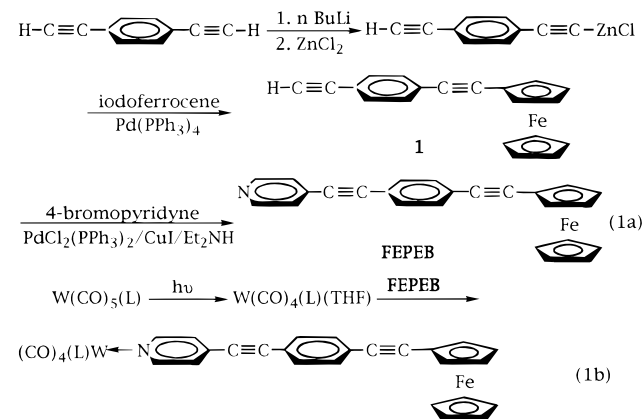
1-(Ferrocenylethynyl)-4-((4-aminophenyl)ethynyl)benzene (18; FEAEB). Pale yellow **18** was synthesized by the same procedures as employed for **16**, except that **17** was utilized instead of **15**. Complex **18** was eluted by THF/hexane (1:5), providing a yield of 55%. Anal. Calcd for C₂₆H₂₉NFe: C, 77.82; H, 4.77; N, 3.49. Found: C, 77.68; H, 4.70; N, 3.39.

Crystallographic Studies. Crystals of **1**, **4**, **8**, and **1,8-bis(ferrocenyl)octatetrayne (19)** were grown by slowly diffusing hexane into a concentrated solution of relevant complexes in CH₂Cl₂. Crystals were mounted in thin-walled glass capillaries. Diffraction was measured by an Enraf-Nonius CAD4 diffractometer with an θ - 2θ scan mode. Unit cells were determined by centering 25 reflections in the appropriate 2θ range. Other relevant experimental details are listed in Table 1. All data reduction and refinements were performed on a MicroVax 3800 computer employing NRCVAX¹⁷ programs. Intensities were collected and corrected for decay, absorption (empirical, ψ -scan), and Lp effects. The structures were solved by a combination of direct methods¹⁸ and difference Fourier methods and further refined by full-matrix least-squares techniques. All non-hydrogen atoms were refined anisotropically, and all hydrogen atoms were included in the structure factor calculation in idealized positions with $d_{C-H} = 0.95$ Å. Because of disorder, atoms C13–C16 and C21–C25 in complex **8** have only 50% occupancy.

Results and Discussion

In this study, three series of complexes, **I**, **II**, and **III**, containing an end-capping ferrocenyl moiety, were synthesized. A palladium(0)-catalyzed coupling of organozinc with iodoferrocene provided 1-(ferrocenyl-

ethynyl)-4-ethynylbenzene (**1**).¹⁹ A Sonogashira coupling²⁰ of **1** and 4-bromopyridine catalyzed by 3 mol % of PdCl₂(PPh₃)₂ and CuI in diethylamine yielded 1-(ferrocenylethynyl)-4-((4-pyridyl)ethynyl)benzene (FEPEB; **2**). Coordinating the dangling pyridine of **2** with W(CO)₄(L)(THF), prepared in situ by photolyzing W(CO)₅(L), led to the formation of heteronuclear dimers **I**, W(CO)₄(L)(FEPEB) (**3**, L = CO; **4**, L = PPh₃; **5**, L = P(OMe)₃; **6**, L = PMe₃) (eq 1). A combination of Cu(I)



and Cu(II) from various sources, with or without the presence of O₂, was observed to effect the oxidative coupling of terminal alkynes.²¹ It was found that combining Cu(OAc)₂ and CuI in oxygen caused the coupling of ferrocenylbutadiyne (or ferrocenylacetylene) and ethynylpyridine to form 1-ferrocenyl-6-(4-pyridyl)-hexatriyne (**7**; FPHT) or 1-ferrocenyl-4-(4-pyridyl)-butadiyne (**12**; FPBD), although the homocoupling products 1,8-bis(ferrocenyl)octatetrayne¹⁶ (or 1,4-diferrocenylbutadiyne¹⁶) and 1,4-bis(4-pyridyl)butadiyne (DPB)¹² were also obtained. Complexes of series **II**, W(CO)₄(L)(FPHT) (**8**, L = CO; **9**, L = PPh₃; **10**, L =

(19) Compound **1** was reported in the literature recently: Hsung, R. P.; Chidsey, S. E. D.; Sita, L. R. *Organometallics* **1995**, *14*, 4808.

(20) Campbell, I. B. In *Organocopper Reagents*; Taylor, R. J. K., Ed.; Oxford University Press: Oxford, U.K., 1994; Chapter 10.

(21) (a) Kozhushkov, S.; Haumann, T.; Boese, R.; Knieriem, B.; Scheib, S.; Bauerle, P.; de Meijere, A. *Angew. Chem., Int. Ed. Engl.* **1995**, *34*, 781. (b) Parshall, G. W.; Ittel, S. D. *Homogeneous Catalysis*, 2nd ed.; Wiley: New York, 1992; pp 194–195. (c) Tabushi, I.; Yuan, L. C.; Shimokawa, K.; Mizutani, T.; Kuroda, Y. *Tetrahedron Lett.* **1981**, *22*, 2273. (d) Hay, A. S. *J. Org. Chem.* **1962**, *27*, 3320.

(17) Gabe, E. J.; LePage, Y.; Charland, J. P.; Lee, F. L.; White, P. S. *J. Appl. Crystallogr.* **1989**, *22*, 384.

(18) Main, P.; Fiske, S. J.; Hull, S. E.; Lessinger, L.; Germain, G.; Declercq, J. P.; Woolfson, M. M. Multan80: A System of Computer Programs for the Automatic Solution of Crystal Structures from X-ray Diffraction Data; Universities of York, U.K., and Louvain, Belgium, 1980.

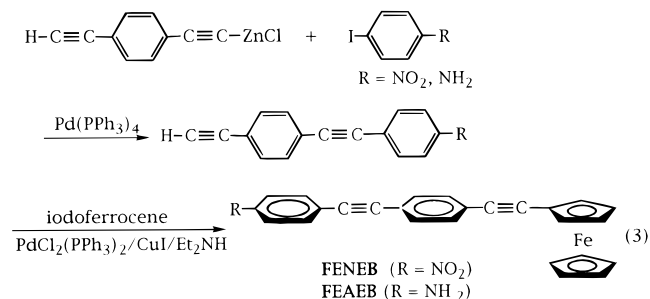
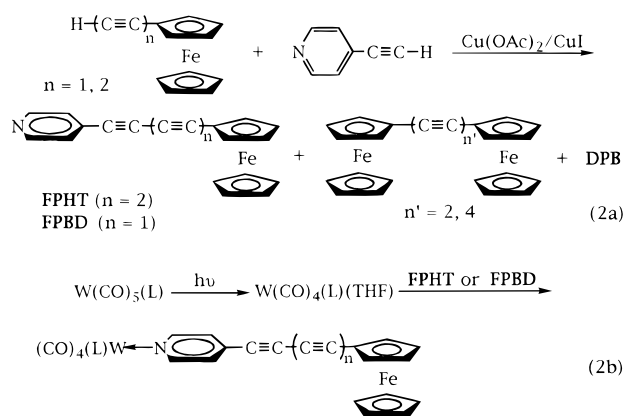
Table 2. IR Spectra in the $\nu(\text{CO})$ Region and ^1H and $^{31}\text{P}\{^1\text{H}\}$ NMR Spectra

compd	$\nu(\text{CO}), \nu(\text{C}\equiv\text{C}),^a$ cm^{-1}	δ , ppm ^{b,c} (J, Hz)	δ , ppm ^{b,d} (J, Hz)
1		8.91 (d, 2 H, $J_{\text{H-H}} = 6.8$, NCH), 8.68 (d, 2 H, $J_{\text{H-H}} = 6.0$, NCH), 7.72 (d, 2 H, $J_{\text{H-H}} = 6.8$, NCHCH), 7.54 (d, 2 H, $J_{\text{H-H}} = 6.0$, NCHCH)	
2		8.57 (d, 2 H, $J_{\text{H-H}} = 5.9$, NCH), 7.53 (d, 2 H, $J_{\text{H-H}} = 8.5$, Ph), 7.47 (d, 2 H, $J_{\text{H-H}} = 8.5$, Ph), 7.38 (d, 2 H, $J_{\text{H-H}} = 5.9$, NCHCH), 4.50 (t, 2 H, $J_{\text{H-H}} = 1.8$, C ₅ H ₄), 4.28 (t, 2 H, $J_{\text{H-H}} = 1.8$, C ₅ H ₄), 4.23 (s, 5 H, C ₅ H ₅)	
3	2072 m, 1972 vw, 1929 s, 1890 sh	9.10 (d, 2 H, $J_{\text{H-H}} = 6.9$, NCH), 7.62 (d, 2 H, $J_{\text{H-H}} = 8.3$, Ph), 7.56 (d, 2 H, $J_{\text{H-H}} = 8.3$, Ph), 7.50 (d, 2 H, $J_{\text{H-H}} = 6.9$, NCHCH), 4.54 (t, 2 H, $J_{\text{H-H}} = 1.8$, C ₅ H ₄), 4.33 (t, 2 H, $J_{\text{H-H}} = 1.8$, C ₅ H ₄), 4.26 (s, 5 H, C ₅ H ₅)	
4	2026 vs, 1925 s, 1891 m	8.54 (d, 2 H, $J_{\text{H-H}} = 6.7$, NCH), 7.60 (d, 2 H, $J_{\text{H-H}} = 8.6$, Ph), 7.54 (d, 2 H, $J_{\text{H-H}} = 8.6$, Ph), 7.45–7.38 (m, 15 H, PPh ₃), 7.14 (d, 2 H, $J_{\text{H-H}} = 6.7$, NCHCH), 4.54 (t, 2 H, $J_{\text{H-H}} = 1.8$, C ₅ H ₄), 4.33 (t, 2 H, $J_{\text{H-H}} = 1.8$, C ₅ H ₄), 4.26 (s, 5 H, C ₅ H ₅)	36.7 (s, $J_{\text{P-W}} = 241$)
5	2019 m, 1893 vs, 1853 s, 2217 w	8.97 (d, 2 H, $J_{\text{H-H}} = 6.5$, NCH), 7.63 (d, 2 H, $J_{\text{H-H}} = 8.6$, Ph), 7.55 (d, 2 H, $J_{\text{H-H}} = 8.6$, Ph), 7.51 (d, 2 H, $J_{\text{H-H}} = 6.5$, NCHCH), 4.54 (t, 2 H, $J_{\text{H-H}} = 1.8$, C ₅ H ₄), 4.33 (t, 2 H, $J_{\text{H-H}} = 1.8$, C ₅ H ₄), 4.26 (s, 5 H, C ₅ H ₅), 3.59 (d, 9 H, OMe)	152 (s, $J_{\text{P-W}} = 341$)
6	2007 m, 1874 vs, 1845 s, 2214 w	9.00 (d, 2 H, $J_{\text{H-H}} = 6.6$, NCH), 7.62 (d, 2 H, $J_{\text{H-H}} = 8.5$, Ph), 7.55 (d, 2 H, $J_{\text{H-H}} = 8.5$, Ph), 7.52 (d, 2 H, $J_{\text{H-H}} = 6.5$, NCHCH), 4.54 (t, 2 H, $J_{\text{H-H}} = 1.8$, C ₅ H ₄), 4.33 (t, 2 H, $J_{\text{H-H}} = 1.8$, C ₅ H ₄), 4.26 (s, 5 H, C ₅ H ₅), 3.59 (d, 9 H, OMe)	-21.5 (s, $J_{\text{P-W}} = 226$)
7		8.64 (d, 2 H, $J_{\text{H-H}} = 5.7$, NCH), 7.50 (d, 2 H, $J_{\text{H-H}} = 5.7$, NCHCH), 4.66 (t, 2 H, $J_{\text{H-H}} = 1.8$, C ₅ H ₄), 4.43 (t, 2 H, $J_{\text{H-H}} = 1.8$, C ₅ H ₄), 4.30 (s, 5 H, C ₅ H ₅)	
8	2071 m, 1965 vw, 1927 s, 1890 sh, 2167 w	9.07 (d, 2 H, $J_{\text{H-H}} = 6.4$, NCH), 7.61 (d, 2 H, $J_{\text{H-H}} = 6.4$, NCHCH), 4.66 (t, 2 H, $J_{\text{H-H}} = 1.8$, C ₅ H ₄), 4.45 (t, 2 H, $J_{\text{H-H}} = 1.8$, C ₅ H ₄), 4.31 (s, 5 H, C ₅ H ₅)	
9^e	2011 m, 1885 vs, 1849 s, 2166 w	8.56 (d, 2 H, $J_{\text{H-H}} = 6.8$, NCH), 7.46–7.38 (m, 15 H, PPh ₃), 7.14 (d, 2 H, $J_{\text{H-H}} = 6.8$, NCHCH), 4.67 (t, 2 H, $J_{\text{H-H}} = 1.8$, C ₅ H ₄), 4.45 (t, 2 H, $J_{\text{H-H}} = 1.8$, C ₅ H ₄), 4.31 (s, 5 H, C ₅ H ₅)	37.0 (s, $J_{\text{P-W}} = 241$)
10^e	2019 m, 1903 vs, 1850 s, 2168 w	8.99 (d, 2 H, $J_{\text{H-H}} = 6.7$, NCH), 7.52 (d, 2 H, $J_{\text{H-H}} = 6.7$, NCHCH), 4.67 (t, 2 H, $J_{\text{H-H}} = 1.8$, C ₅ H ₄), 4.44 (t, 2 H, $J_{\text{H-H}} = 1.8$, C ₅ H ₄), 4.31 (s, 5 H, C ₅ H ₅), 3.61 (d, 9 H, $J_{\text{P-H}} = 11.0$, OMe)	153 (s, $J_{\text{P-W}} = 384$)
11^e	2007 m, 1874 vs, 1846 s, 2165 w	9.03 (d, 2 H, $J_{\text{H-H}} = 6.6$, NCH), 7.51 (d, 2 H, $J_{\text{H-H}} = 6.6$, NCHCH), 4.67 (t, 2 H, $J_{\text{H-H}} = 1.8$, C ₅ H ₄), 4.44 (t, 2 H, $J_{\text{H-H}} = 1.8$, C ₅ H ₄), 4.29 (s, 5 H, C ₅ H ₅), 1.50 (d, 9 H, $J_{\text{P-H}} = 7.5$, Me)	-21.8 (s, $J_{\text{P-W}} = 233$)
12		8.61 (d, 2 H, $J_{\text{H-H}} = 5.1$, NCH), 7.46 (d, 2 H, $J_{\text{H-H}} = 5.1$, NCHCH), 4.62 (t, 2 H, $J_{\text{H-H}} = 1.8$, C ₅ H ₄), 4.40 (t, 2 H, $J_{\text{H-H}} = 1.8$, C ₅ H ₄), 4.29 (s, 5 H, C ₅ H ₅)	
13	2070 m, 1932 s, 1897 m	9.04 (d, 2 H, $J_{\text{H-H}} = 5.1$, NCH), 7.56 (d, 2 H, $J_{\text{H-H}} = 5.1$, NCHCH), 4.65 (t, 2 H, $J_{\text{H-H}} = 1.8$, C ₅ H ₄), 4.43 (t, 2 H, $J_{\text{H-H}} = 1.8$, C ₅ H ₄), 4.30 (s, 5 H, C ₅ H ₅)	
14		9.24 (d, 2 H, $J_{\text{H-H}} = 6.4$, NCH), 8.33 (d, 2 H, $J_{\text{H-H}} = 6.6$, NCHCH), 4.70 t, 2 H, $J_{\text{H-H}} = 1.8$, C ₅ H ₄), 4.64 (s, 3 H, NCH ₂), 4.49 (t, 2 H, $J_{\text{H-H}} = 1.8$, C ₅ H ₄), 4.33 (s, 5 H, C ₅ H ₅)	
15		8.29 (d, 2 H, $J_{\text{H-H}} = 8.4$, CHCNO ₂), 7.84 (d, 2 H, $J_{\text{H-H}} = 8.4$, CHCNO ₂), 7.66 (d, 2 H, $J_{\text{H-H}} = 8.7$, C ₆ H ₄), 7.58 (d, 2 H, $J_{\text{H-H}} = 8.7$, C ₆ H ₄), 3.82 (s, 1 H, ≡CH)	
16^e		8.31 (d, 2 H, $J_{\text{H-H}} = 8.8$, CHCNO ₂), 7.96 (d, 2 H, $J_{\text{H-H}} = 8.8$, CHCNO ₂), 7.60 (d, 2 H, $J_{\text{H-H}} = 8.3$, C ₆ H ₄), 7.54 (d, 2 H, $J_{\text{H-H}} = 8.3$, C ₆ H ₄), 4.56 (t, 2 H, $J_{\text{H-H}} = 1.8$, C ₅ H ₄), 4.33 (t, 2 H, $J_{\text{H-H}} = 1.8$, C ₅ H ₄), 4.29 (s, 5 H, C ₅ H ₅)	
17		7.47 (s, 4 H, Ph), 7.24 (d, 2 H, $J_{\text{H-H}} = 6.6$, CHCHNH ₂), 6.66 (d, 2 H, $J_{\text{H-H}} = 6.6$, CHNH ₂), 5.05 (br s, 2 H, NH ₂)	
18^e		7.45 (d, 2 H, $J_{\text{H-H}} = 8.7$, C ₆ H ₄), 7.42 (d, 2 H, $J_{\text{H-H}} = 8.7$, C ₆ H ₄), 7.20 (d, 2 H, $J_{\text{H-H}} = 8.4$, CHCHNH ₂), 6.55 (d, 2 H, $J_{\text{H-H}} = 8.4$, CHCNO ₂), 5.61 (s, 2 H, NH ₂), 4.57 (t, 2 H, $J_{\text{H-H}} = 1.8$, C ₅ H ₄), 4.34 (t, 2 H, $J_{\text{H-H}} = 1.8$, C ₅ H ₄), 4.26 (s, 5 H, C ₅ H ₅)	

^a Measured in CH₂Cl₂ solution. ^b Measured in acetone-*d*₆ except for **2**, **3**, and **5**, which were measured in CDCl₃. ^c Reported in ppm relative to $\delta(\text{Me}_4\text{Si})$ at 0 ppm. ^d Reported in ppm relative to $\delta(85\% \text{H}_3\text{PO}_4)$ at 0 ppm. ^e The signals due to the AA'MM' spin system in symmetrical Cp ligands are, due to their simple appearance, reported as triplets with coupling constants equal to half of the separation between the two outer lines. Abbreviations: s = singlet, d = doublet, t = triplet, m = multiplet.

P(OMe)₃; **11**, L = PMe₃) and W(CO)₅(FPBD) (**13**), were synthesized from the reactions of W(CO)₄(L) with **7** and **12**, respectively (eq 2). 1-Ethynyl-4-((4-nitrophenyl)-

ethynyl)benzene (**18**; FEAEB), were obtained from a subsequent Sonogashira coupling reaction between iodoferrocene and **15** (or **17**) (eq 3).



ethynyl)benzene (**15**) and 1-ethynyl-4-((4-aminophenyl)-ethynyl)benzene (**17**) were synthesized from a palladium(0)-catalyzed coupling of organozinc derived from 1,4-diethylbenzene with 4-iodo-1-nitrobenzene and 4-iodoaniline, respectively. The complexes of series **III**, 1-(ferrocenylethynyl)-4-((4-nitrophenyl)ethynyl)benzene (**16**; FENEB) and 1-(ferrocenyl-4-((4-aminophenyl)-

The spectroscopic properties (Table 2) of these new complexes correlate with their formulations. Three moderate/strong carbonyl stretching bands for **4–6** and **9–11** in the infrared spectra require that the phosphorus donor ligand and pyridine be mutual by cis at the tungsten center. Except for **4** and **9**, the α -ring protons of pyridines for the complexes have the chemical shifts appearing at lower field than those of free ligands in the ¹H NMR spectra. The lower δ values for the α -ring protons of pyridine in **4** and **9** probably arise from the ring current shielding caused by the phenyl ligand of

Table 3. UV Spectra and Assignments in CH₂Cl₂

compd	λ_{\max} , nm	
	$\pi-\pi^*$	MLCT
1	310	
2	316	
3	330	395
4	330	437
5	330	404
6	330	454
7	318, 340, 365	
8	330, 358	425
9	325, 348, 370	487
10	325, 348	460
11		505
12	315, 335, 370	
13	305, 325, 335	402
14	315, 350, 375	558
16	348	
18	335	

the triphenylphosphine. A singlet accompanied by a pair of tungsten satellites with $^1J_{P-W} = 226-384$ Hz is observed in the ^{31}P NMR spectra for all complexes containing a coordinated phosphine or phosphite.

Table 3 illustrates the electronic spectra of the new complexes in CH₂Cl₂ at room temperature. The $\pi \rightarrow \pi^*$ transition bands were assigned according to the various ferrocenyl complexes²² and the tungsten to pyridine charge-transfer (MLCT) transition bands assigned according to the relevant tungsten carbonyl pyridyl complexes.²³ In accordance with what previous literature has reported, these MLCT bands fall in the range of 390–490 nm²⁴ and exhibit a hypsochromic shift as the solvent polarity increases.²⁵ The ancillary ligands strongly influence the MLCT energies of the complexes, and the MLCT energies in turn are ordered in accordance with the π -accepting ability of the ligands; L = CO > P(OMe)₃ > PPh₃ > PMe₃. The much weaker d–d transition substantially overlap the MLCT bands and are not assigned. The intense $\pi \rightarrow \pi^*$ transition associated with conjugated alkynyl ligands for **1** ($\lambda = 310$ nm) and **2** ($\lambda = 316$ nm) is not observed in ferrocenylacetylene in the same region, possibly because elongating the conjugation length lowers the energy of the π^* orbital. The extra pyridine moiety in **2** increases the λ_{\max} value by 6 nm compared to the value for **1**. Coordinating the dangling pyridine of **2** with W(CO)₄(L), an inductive acceptor,^{6a} further increases the λ_{\max} value by 14 nm. The spectra of compounds **7** and **12** are more complicated than that of ferrocenyl-4-pyridylacetylene

Table 4. Redox Potentials for Complexes in CH₂Cl₂/CH₃CN (1:1) at 298 K^a

complex	$E_{\text{ox}} (\Delta E_p)/\text{Fe}(2+/3+);$ W(1+/2+)	$E_{\text{red}} (\Delta E_p)/$ (PY(0/1-))
1 , EFEB	+0.19 (77)	
2 , FEPEB	+0.18 (80)	-2.00 (i)
3 , W(CO) ₅ (FEPEB)	+0.14 (80); +0.70 (i)	-2.02 (i)
4 , W(CO) ₄ (PPh ₃)(FEPEB)	+0.15 (86); +0.36 (i)	-2.04 (i)
5 , W(CO) ₄ (P(OMe) ₃)(FEPEB)	+0.20 (76); +0.46 (i)	-2.05 (i)
6 , W(CO) ₄ (PMe ₃)(FEPEB)	+0.23 (overlapping)	-2.06 (i)
7 , FPHT	+0.22 (90)	-2.14 (i)
8 , W(CO) ₅ (FPHT)	+0.22 (110); +0.70 (i)	-1.78 (130); -2.22 (140)
9 , W(CO) ₄ (PPh ₃)(FPHT)	+0.26 (overlapping)	-1.79 (110); -2.26 (110)
10 , W(CO) ₄ (P(OMe) ₃)(FPHT)	+0.24 (80); +0.39 (i)	-1.82 (105); <-2.50
11 , W(CO) ₄ (PMe ₃)(FPHT)	+0.20 (91, overlapping)	-1.78 (i); <-2.50
12 , FPBD	+0.20 (94)	-2.10 (i)
13 , W(CO) ₅ (FPBD)	+0.22 (92)	-1.60 (i)
14 , FPHTI	+0.25 (80)	-2.07 (i)
16 , FENEB	+0.14 (78), +0.28 (60)	-1.44 (120), -2.30 (130)
18 , FEAEB	+0.18 (i), +0.68 (i)	<-2.50

^a Analyses performed in 10⁻³ M deoxygenated CH₂Cl₂/CH₃CN (1:1) solutions containing 0.1 M TBAP; the scan rate is 100 mV. All potentials in volts vs ferrocene (0.00 V with peak separation of 81 mV in CH₂Cl₂/CH₃CN (1:1)); scan range +1.5 to -2.5 V; i = irreversible process; $\Delta E_p = E_{\text{pa}} - E_{\text{pc}}$ (mV).

(FPA) due to the conjugated system located on the polyne fragment.²⁶ Notably, a strong low-lying band, attributable to charge-transfer transition, is observed for derivatives of **7** ($\lambda = 558$ nm) and **12** ($\lambda = 554$ nm) if the pendant pyridine is converted to *N*-methylpyridinium, which is a good electron acceptor.²⁷ Replacing the amino group in **18** ($\lambda = 335$ nm) by a strong π acceptor causes only a slight increase in λ (348 nm, **16**). The λ_{\max} values of several ferrocene-terminated phenylethynyl oligomers, Cp₂Fe-[C≡C-C₆H₄]_n-X, were also observed to be rather insensitive to variations of X.¹⁹

The oxidation potentials (Table 4) of tungsten atoms in the complexes W(CO)₄(L)(FEPEB) and W(CO)₄(L)(FPHT) share certain common features with complexes W(CO)₄(L)(PY) (PY = conjugated pyridines), as has been previously reported:^{2b} (1) the oxidation process is irreversible; (2) the oxidation potentials in the same series of complexes are ordered L = CO > P(OR)₃ > PPh₃ > PMe₃; (3) within the same series of complexes, a complex with L = CO exhibits a significantly higher oxidation potential than any with an L = phosphorus donor ligand. Except for complex **18**, the iron atoms in all the complexes were found to possess a reversible oxidation potential, which appeared at more positive values (0.15–0.25 eV) than ferrocene. This phenomenon resembles that observed for the complexes Cp₂Fe-[C≡C-C₆H₄]_n-X¹⁹ and may be attributable to the presence of a somewhat electron withdrawing alkyne unit in the cyclopentadienyl ligand.

The reduction potentials for PY π^* levels of the complexes are consistent with the energy stabilization obtained by the π^* acceptor orbital upon ligation of PY.

(26) (a) Hoshi, T.; Okubo, J.; Kobayashi, M.; Tanizaki, Y. *J. Am. Chem. Soc.* **1986**, *108*, 3867. (b) Steigman, A. E.; Miskowski, V. M.; Perry, J. W. *J. Am. Chem. Soc.* **1987**, *109*, 5884. (c) Kobayashi, M.; Hoshi, T.; Okubo, J.; Hiratsuka, H.; Harazono, T.; Nakagawa, M.; Tanizaki, Y. *Bull. Chem. Soc. Jpn.* **1984**, *108*, 3867.

(27) (a) Marder, S. R.; Perry, J. W.; Yakymyshyn, C. P. *Chem. Mater.* **1994**, *6*, 1137. (b) Marder, S. R.; Perry, J. W.; Tiemann, B. G.; Schaefer, W. P. *Organometallics* **1991**, *10*, 1896.

(22) (a) Alain, V.; Fort, A.; Barzoukas, M.; Chen, C. T. *Inorg. Chim. Acta* **1996**, *242*, 43. (b) Calabrese, J. C.; Cheng, L. T.; Green, J. C.; Marder, S. R.; Tam, W. *J. Am. Chem. Soc.* **1991**, *113*, 7227. (c) Toma, S.; Gaplovsky, A.; Elecko, P. *Chem. Pap.* **1985**, *39*, 115. (d) Sohn, Y. S.; Hendrickson, D. N.; Gray, H. B. *J. Am. Chem. Soc.* **1971**, *93*, 3603. (e) Rosenblum, M.; Brawn, N.; Papenmeier, J.; Applebaum, M. *J. Organomet. Chem.* **1966**, *6*, 173.

(23) (a) Zulu, M. M.; Lees, A. J. *Inorg. Chem.* **1988**, *27*, 1139. (b) Lees, A. J.; Fobare, J. M.; Mattimore, E. F. *Inorg. Chem.* **1984**, *23*, 2709. (c) Gaus, P. L.; Boncella, J. M.; Rosengren, K. S.; Funk, M. O. *Inorg. Chem.* **1982**, *21*, 2174. (d) Pannel, K. H.; Gonzalez, M. G. d. I. P. S.; Leano, H.; Iglesias, R. *Inorg. Chem.* **1978**, *17*, 1093. (e) Wrighton, M. S.; Abrahamson, H. B.; Morse, D. L. *J. Am. Chem. Soc.* **1976**, *98*, 4105.

(24) (a) Zulu, M. M.; Lees, A. J. *Inorg. Chem.* **1988**, *27*, 1139. (b) Lees, A. J.; Fobare, J. M.; Mattimore, E. F. *Inorg. Chem.* **1984**, *23*, 2709. (c) Gaus, P. L.; Boncella, J. M.; Rosengren, K. S.; Funk, M. O. *Inorg. Chem.* **1982**, *21*, 2174. (d) Pannel, K. H.; Gonzalez, M. G. d. I. P. S.; Leano, H.; Iglesias, R. *Inorg. Chem.* **1978**, *17*, 1093. (e) Wrighton, M. S.; Abrahamson, H. B.; Morse, D. L. *J. Am. Chem. Soc.* **1976**, *98*, 4105.

(25) Kaim, W.; Kuhlmann, S.; Olbrich-Deussner, B.; Bessen-bacher, C.; Schulz, A. *J. Organomet. Chem.* **1987**, *321*, 215.

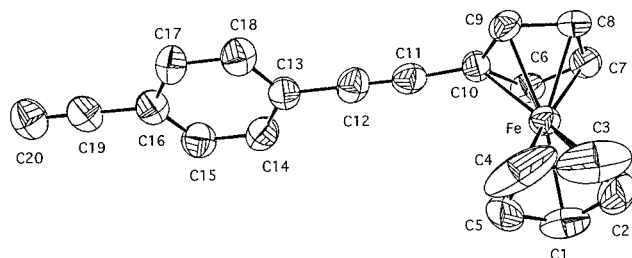


Figure 1. ORTEP diagram of complex **1**. Thermal ellipsoids are drawn with 30% probability boundaries.

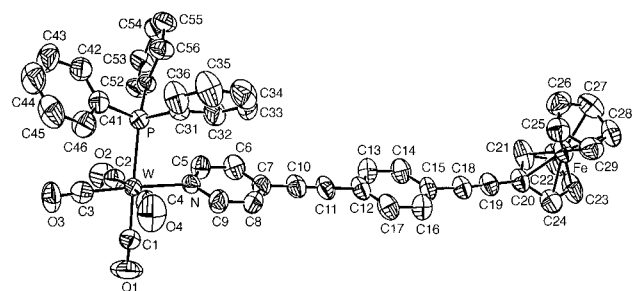


Figure 2. ORTEP diagram of complex **4**. Thermal ellipsoids are drawn with 30% probability boundaries.

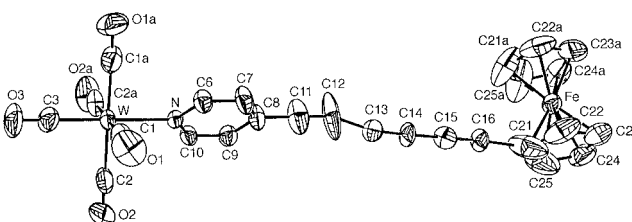


Figure 3. ORTEP diagram of complex **8**. Thermal ellipsoids are drawn with 30% probability boundaries.

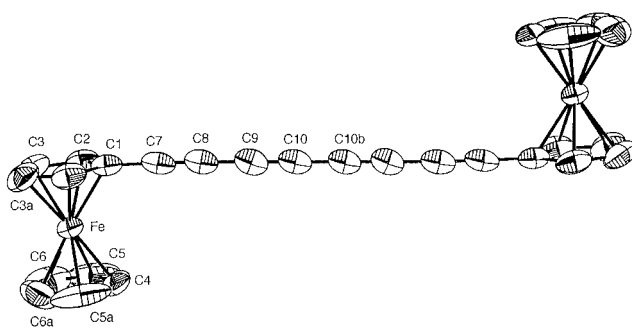


Figure 4. ORTEP diagram of complex **19**. Thermal ellipsoids are drawn with 30% probability boundaries.

Molecular Structures of 1-(Ferrocenylethynyl)-4-ethynylbenzene (1), W(CO)₄(PPh₃)(FEPEB) (4), W(CO)₅(FPHT) (8), and 1,8-Bis(ferrocenyl)octatetrayne (19). The ORTEP drawings of **1**, **4**, **8**, and **19** are displayed in Figures 1–4, respectively. Table 5 lists selected bond distances and angles for the complexes. The coordination core surrounding the tungsten atom in **4** and **8** almost configures an octahedron, and in **4**, the pyridyl ligand is cis to the phosphine ligand. In order for d_{xz} and d_{yz} orbitals to participate effectively in the metal to pyridyl π^* charge transfer (N–W–C₃ is assumed to be the z axis), the dihedral angle between the pyridyl ring (plane A) and the best constituted plane of W, N, C₂, C₃, and C₄ (or W, N, C_{2a}, C₃, and C₁) (plane B) should be 0, 45, or 90°. Complex **4** significantly deviates from these ideal angles (the largest deviations of atoms from the least-squares planes A and

Table 5. Selected Bond Distances (Å) and Angles (deg) for Complexes **1**, **4**, **8**, and **19**

	1	4	8	19
Distances				
W–P	2.560(2)			
W–N	2.268(5)		2.277(8)	
W–C ₁	1.960(8)		2.02(1)	
W–C ₂	2.032(8)		2.03(1)	
W–C ₃	1.954(8)		1.98(1)	
W–C ₄	2.008(8)			
Fe–C ₁	2.040(5)			2.032(5)
Fe–C ₂	2.027(6)			2.024(4)
Fe–C ₃	2.011(7)			2.032(4)
Fe–C ₄	2.020(7)			2.00297
Fe–C ₅	2.017(5)			2.001(5)
Fe–C ₆	2.039(5)			1.990(5)
Fe–C ₇	2.032(5)			
Fe–C ₈	2.036(5)			
Fe–C ₉	2.036(5)			
Fe–C ₁₀	2.043(5)			
Fe–C ₂₀		2.030(7)		
Fe–C ₂₁		2.048(8)	2.01(1)	
Fe–C ₂₂		2.028(8)	2.02(1)	
Fe–C ₂₃		2.031(9)	2.02(1)	
Fe–C ₂₄		2.033(8)	2.02(1)	
Fe–C ₂₅		2.035(8)	2.00(1)	
Fe–C ₂₆		2.044(9)		
Fe–C ₂₇		2.033(8)		
Fe–C ₂₈		2.037(8)		
Fe–C ₂₉		2.046(8)		
C ₁ –O ₁		1.15(1)	1.14(1)	
C ₂ –O ₂		1.14(1)	1.13(1)	
C ₃ –O ₃		1.16(2)	1.15(2)	
C ₄ –O ₄		1.14(1)		
N–C ₅		1.332(9)		
N–C ₆			1.33(1)	
N–C ₉		1.36(1)		
N–C ₁₀			1.32(1)	
C ₇ –C ₈				1.19(1)
C ₉ –C ₁₀				1.188(9)
C ₁₀ –C ₁₁		1.19(1)		
C ₁₁ –C ₁₂	1.189(8)		1.18(2)	
C ₁₃ –C ₁₄			1.21(2)	
C ₁₅ –C ₁₆			1.20(2)	
C ₁₉ –C ₂₀	1.170(8)			
Angles				
C ₁ –W–C ₂		85.1(3)	87.9(4)	
C ₁ –W–C ₃		86.1(3)	89.8(4)	
C ₁ –W–C ₄		88.1(3)		
C ₁ –W–C _{1a}			91.7(4)	
C ₂ –W–C _{2a}			92.6(4)	
C ₁ –W–P		175.4(2)		
C ₁ –W–N		91.5(2)	89.0(3)	
C ₂ –W–C ₃		87.8(3)	90.8(4)	
C ₂ –W–C ₄		171.0(3)		
C ₂ –W–P		99.4(2)		
C ₂ –W–N		92.3(2)	90.4(3)	
C ₂ –W–N ₁				
C ₃ –W–C ₄		85.8(3)		
C ₃ –W–P		94.4(2)		
C ₃ –W–N		177.6(3)	178.3(4)	
C ₄ –W–P		87.4(2)		
C ₄ –W–N		93.8(2)		
W–C ₁ –O ₁		177.1(7)	177.9(8)	
W–C ₂ –O ₂		175.2(6)	178.3(7)	
W–C ₃ –O ₃		176.1(7)	177(1)	
W–C ₄ –O ₄		174.9(7)		
P–W–N		87.9(1)		
C ₁ –C ₇ –C ₈				179.5(5)
C ₇ –C ₈ –C ₉				177.9(6)
C ₈ –C ₉ –C ₁₀				179.6(6)
C ₉ –C ₁₀ –C _{10b}				179.6(6)
C ₇ –C ₁₀ –C ₁₁		176.9(9)		
C ₈ –C ₁₁ –C ₁₂			179(1)	
C ₁₀ –C ₁₁ –C ₁₂	175.8(6)	178.0(9)		
C ₁₁ –C ₁₂ –C ₁₃	176.7(6)		155.9(7)	
C ₁₃ –C ₁₄ –C ₁₅			178(2)	
C ₁₄ –C ₁₅ –C ₁₆			177(2)	
C ₁₅ –C ₁₆ –C ₂₁			171(2)	
C ₁₅ –C ₁₈ –C ₁₉		174.4(9)		
C ₁₈ –C ₁₉ –C ₂₀		176.3(8)		
C ₁₆ –C ₁₉ –C ₂₀	179.8(7)			

B are 0.075(4) and 0.01(1) Å, respectively; dihedral angle 21.7(3)°. The dihedral angle for **8** closely approximates the ideal angle (the largest deviations of atoms from the least-squares planes A and B are 0.00(1) and 0.03(1) Å, respectively; dihedral angle 45.8(4)°). Retaining the planarity of the backbone in the bridge is regarded as crucial to the conjugation of π electrons through the bridge. Only **16** has perfect coplanarity for the two Cp rings. Other complexes appear to differ in the degree that the aromatic rings deviate from planarity: for **1**, the dihedral angle of Cp/Ph is 8.6(2)°, and the largest deviations of atoms from the least-squares planes are 0.002(7) and 0.007(7) Å for Cp and Ph, respectively; for **4**, the dihedral angles of py/Ph and Ph/Cp are 2.5(3) and 17.8(4)°, and the largest deviations of atoms from the least-squares planes are 0.00(1) and 0.01(1) Å for Ph and Cp, respectively. Therefore, information regarding just how effective the delocalization of the metal to ligand charge transfer through the bridge proved to be was not accessible from the solid-state structural data.

The W–C–O linkage (174.9(7)–178.3(7)°) does not significantly deviate from linearity. The carbonyl W–C distances range from 1.954(8) to 2.03(1) Å, and as expected, the two mutual trans carbonyl ligands project slightly longer W–C distances. Other relevant crystal data also appear to be normal: the W–P distance is 2.560(2)°; the alkynyl C≡C distances range from 1.170(8)

to 1.21(2) Å. A structural analysis of the series of molecules $\text{NH}_2\text{C}_6\text{H}_4(\text{C}\equiv\text{C})_n\text{C}_6\text{H}_4\text{NO}_2$ ($n = 0-3$) confirmed that charge-transfer interactions through the conjugated backbone gave rise to quinonoid distortions of the nitrophenyl and aminophenyl functional groups, but not of the acetylene bridges.²⁸ No apparent bond alternation in the pyridyl ring or acetylene linkers in **8** was observed. The W–N distances (2.268(5)–2.277(8) Å) are also comparable to the values recorded in the previous literature.²⁹

Acknowledgment. We wish to thank Academia Sinica and the National Science Foundation of the Republic of China for financially supporting this research under Grant no. NSC-85-2113-M-001-034.

Supporting Information Available: Listings of all bond distances and angles, positional parameters, anisotropic and isotropic thermal parameters, and dihedral angles between the least-squares planes and stereoviews for complexes **1**, **4**, **8**, and **19** (29 pages). Ordering information is given on any current masthead page.

OM960607H

(28) Graham, E. M.; Miskowski, V. M.; Perry, J. W.; Coulter, D. R.; Stiegman, A. E.; Schaefer, W. P.; Marsh, R. E. *J. Am. Chem. Soc.* **1989**, *111*, 8772.

(29) Lin, J. T.; Huang, P. S.; Tsai, T. Y. R.; Liao, C. Y.; Tseng, L. H.; Wen, Y. S.; Shi, F. K. *Inorg. Chem.* **1992**, *31*, 4444.